First observation of the direct detection of $D^+ \to \bar{K}^0_L \, \pi^+ \, \pi^- \, \pi^+$ and $D^- \to K^0_L \, \pi^- \, \pi^+ \, \pi^-$ with the Fermilab FOCUS Experiment

Abstract

In this thesis the decays $D^+ \to \bar{K}^0 \, \pi^+ \, \pi^- \, \pi^+$ and $D^- \to K^0 \, \pi^- \, \pi^+ \, \pi^-$ are reconstructed in both the K^0_L and K^0_S states with data taken from the Fermilab FOCUS experiment. This constitutes a first observation of the direct detection of these decays in the K^0_L mode. We detail the cuts necessary to find the branching ratios of $\Gamma(D^+ \to \bar{K}^0_L \, \pi^+ \, \pi^- \, \pi^+)/ \Gamma(D^+ \to K^0_S \, \pi^+ \, \pi^- \, \pi^+)$ and $\Gamma(D^- \to K^0_L \, \pi^- \, \pi^+ \, \pi^-)/ \Gamma(D^- \to K^0_S \, \pi^- \, \pi^+ \, \pi^-)$, show the branching ratio to be 0.89, and detail further work that remains to be done. The K^0_L is reconstructed using the D^+ flight direction, the direction of the charged pions, and the energy deposited in the hadron calorimeter. The K^0_S decay is reconstructed directly using tracking information in the decay mode $K^0_S \to \pi^+ \, \pi^-$.

A Thesis Presented to the Faculty of the Vanderbilt Physics Department

By Cameron Stewart

April 2014

Acknowledgements

This thesis would not have been possible without Professor Will Johns, my research advisor, who invested the time to teach me about particle physics and data analysis, patiently allowed me to learn from my numerous mistakes throughout the process of this research, and helped to fix computer hardware issues which otherwise would have brought everything to a halt. Furthermore, the large amount of Monte Carlo data used in this analysis was generated with the help of Professor Paul Sheldon who taught me how to use the ACRRE computer cluster and secured for me extra disk space to store the Monte Carlo data. Lastly, I want to thank Professor Med Webster for informing me about honors research and guiding me through the steps of getting my research approved for honors credit.

Chapter 1
Table of Contents:

1 Introduction

1.1 The FOCUS Equipment

The data analyzed in this paper was collected from FOCUS , also called E831, a heavy-flavor photoproduction experiment located in the Wide Band Area of Fermilab that collected data from 1996-1997. It was an upgraded version of the earlier E687 experiment. In FOCUS, a forward multi-particle spectrophotometer was used to measure D mesons and their decay products created from the interaction of a high energy photon beam on a segmented BeO target. The beam was derived from the bremsstrahlung of secondary electrons and positrons from Fermilab's 800 GeV/c Tevatron proton accelerator, creating photons with an endpoint lab-momentum of 300 GeV/c.

Concerning the analysis performed in this thesis, the most important features of the spectrophotometer are that it could: measure the location of the primary vertex where a $D^{\pm}$ was created, measure the location of the secondary vertex where the $D^{\pm}$ decayed, measure the momentum vector of charged decay products with relatively high resolution, distinguish between positive and negative charged particles, and measure the energy deposited in the hadron calorimeter with relatively low spatial resolution.
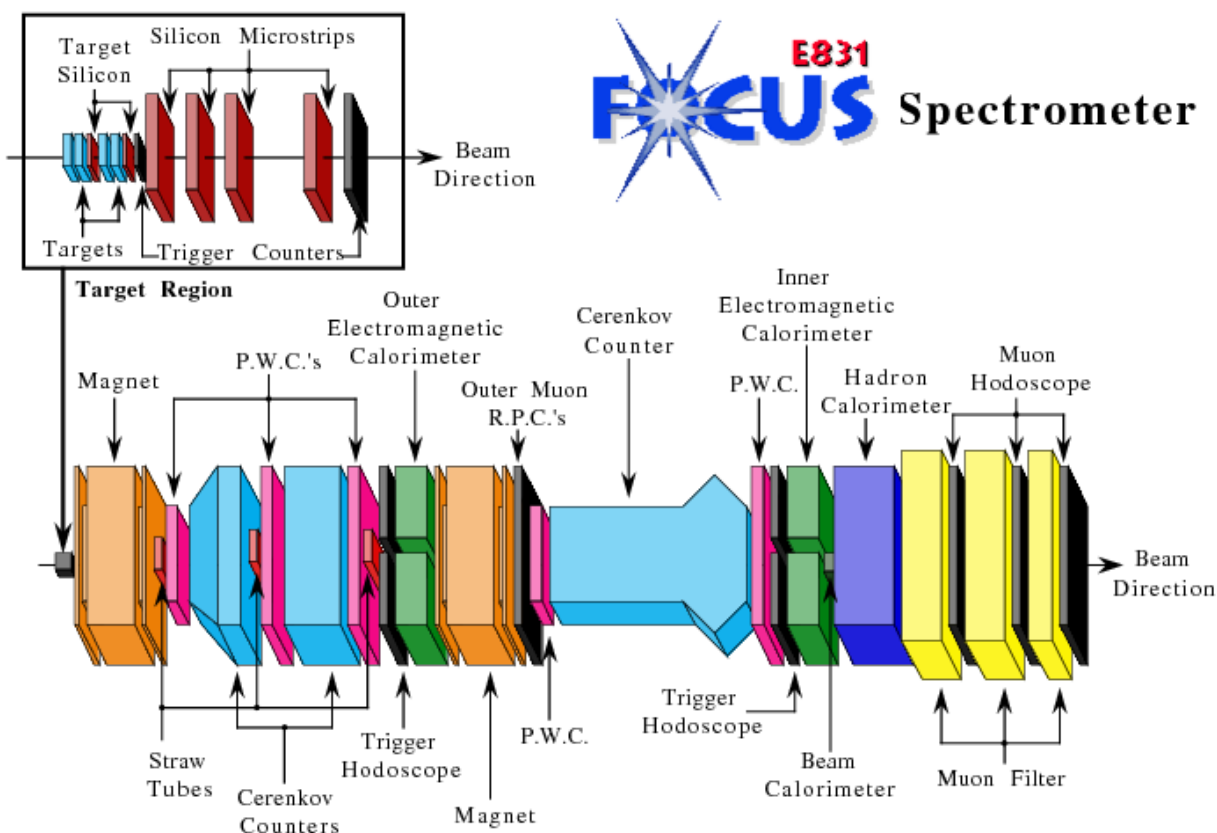

Fig 1.1. A schematic drawing of the FOCUS spectrometer. The inset displays the segmented targets, the embedded target silicon, the trigger counters, and the 12 plane silicon tracking array. The spectrometer is about 30 meters long. [1]

The reconstruction of the primary, production vertex (i.e. $D^{*+} -> D^+ \pi^0$) and secondary, decay vertex (i.e. $D^+ -> K^0_L \pi^+ \pi^- \pi^+$) was performed using information from four silicon microvertex detectors interleaved in the BeO target with two views in two stations followed downstream by twelve planes of microstrips arranged in three views in four stations. The charge to momentum ratio of the particles was measured by the deflection of their paths caused by the two oppositely aligned analysis magnets. Five proportional wire chambers (PWC) were used to track the position of the charged particles which pass through them. Straw tubes supplement tracking in the central pair region. Three multi-cell Cerenkov counters produce light if charged particles are above a certain threshold velocity as shown in figure 1.2. The outer electromagnetic calorimeter covered the outer angle traversed by particles which pass the first magnet but not the second, and the inner electromagnetic calorimeter covered the inner region for particles which pass both magnets. The hadron calorimeter provided low resolution information on the energy deposited by the hadrons. A more complete review of the spectrometer can be found in references [1-2].

Counter	Gas	Thresh (GeV/c)			No. cells
		Pion	Kaon	Proton	
C2	N_2O	4.5	15.9	30.2	110
C1	He–N_2	8.4	29.7	56.5	90
C3	He	17.4	61.5	117	100

Fig. 1.2 Cerenkov counters. [3]

1.2 Relevant Background Information about the D, K, and π mesons

The D meson has several modes of decay. The most similar decay to the $D^+ -> K^0_L \pi^+ \pi^- \pi^+$ mode of decay is $D^+ -> K^0_S \pi^+ \pi^- \pi^+$, which occurs in (3.02±0.12) % of D^+ decays[4]. The branching ratio of K^0_S/ K^0_L in this decay is expected to be close to 1, but this has not been experimentally demonstrated. The K^0_S is more precisely detected than the K^0_L by the low-resolution hadron calorimeter because the K^0_S decays into a π^+ and π^- (69.20±0.05)% of the time and a π^0 and π^0 (30.69±0.05)% of the time before reaching the hadron calorimeter, and the precision reconstruction of the two pions combines to give a higher resolution mapping of the K^0_S path[1]. The time dilation associated with the high energy of the D meson enables the K^0_L to strike the hadron calorimeter before decaying. The D mesons are produced at ~60-70GeV, so the ~2GeV/c^2 D meson experiences a relativistic boost of about 30. It therefore takes it approximately 30m/30c ~ 0.33*10^{-8}s for its decay products to reach the hadron calorimeter in the particle frame. More background information of the mass and mean lifetime of the particles measured in this thesis is given below.

Table 1, Background Information

Particle Name	Particle Symbol	Antiparticle Symbol	Quark content	Rest Mass (MeV/c^2)	Mean lifetime (s)
D meson [4]	D$^+$	D$^-$	c$\bar{\text{d}}$	1,869.62±0.20	1.040 ± 0.007 x 10^{-12}
Pion [5]	π$^+$	π$^-$	u$\bar{\text{d}}$	139.57018 ± 0.00035	2.6033 ± 0.0005 x 10^{-8}
K-Short[6]	K^0_S	Self	$\frac{\text{d}\bar{\text{s}}-\text{s}\bar{\text{d}}}{\sqrt{2}}$	497.614 ± 0.024	(8.954 ± 0.004) x 10^{-11}
K-Long[7]	K^0_L	Self	$\frac{\text{d}\bar{\text{s}}+\text{s}\bar{\text{d}}}{\sqrt{2}}$	497.614 ± 0.024	(5.116 ± 0.021) x 10^{-8}

1.3 Event Reconstruction

The momentum direction of the D$^+$ is measured by the silicon microvertex strips. The momentum of the charged decay products is measured as they are bent by the magnets and tracked by the PWCs. Their velocities are partially known by whether or not they exceed the threshold velocities of the Cerenkov detectors. With the D$^+$ direction known and the pion momentums known, an estimate can be made of the K^0_L momentum and used to improve the low spatial resolution mapping of the hadron calorimeter.
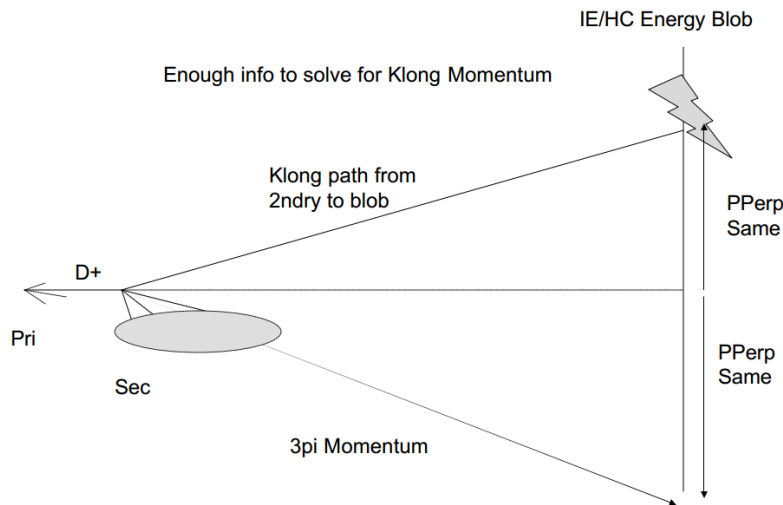

Fig 1.3 This image shows how the D$^+$ direction combined with the 3 pi momentum can be used to improve the estimate of the K_L momentum. Although the kaon momentum is unknown, momentum transverse (PPerp) to the D must balance, and a distinct deposition of energy in the calorimetry allows us to reconstruct the kaon direction. From the PPerp and kaon direction, we can infer the kaon momentum.
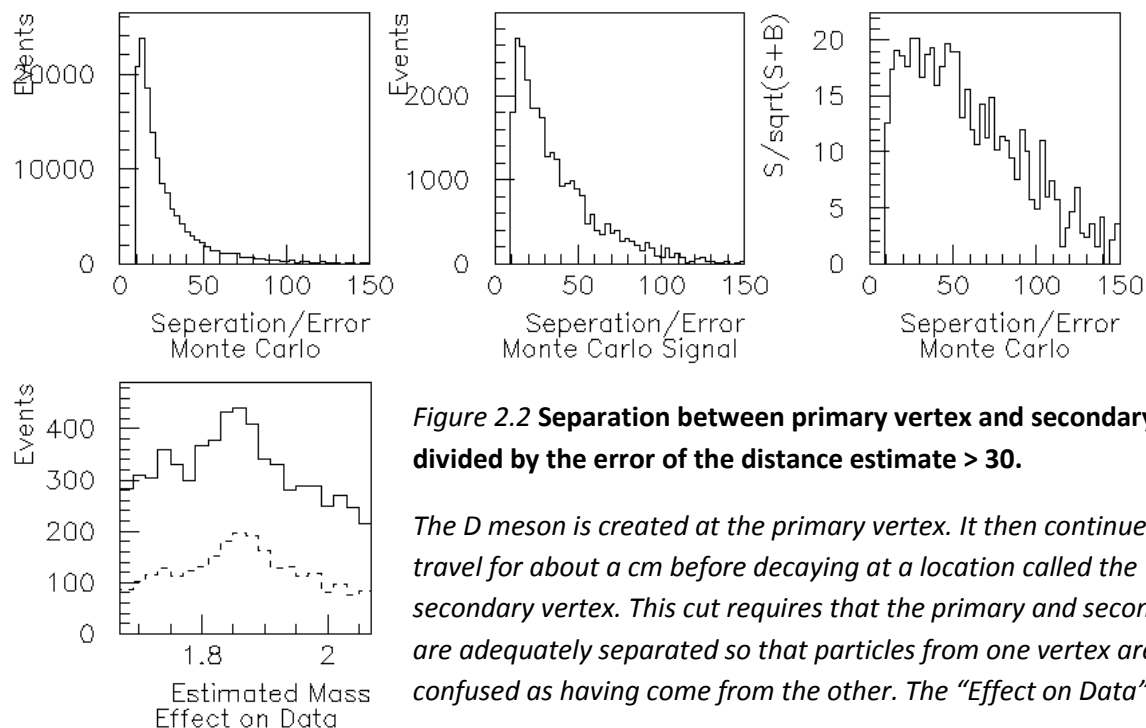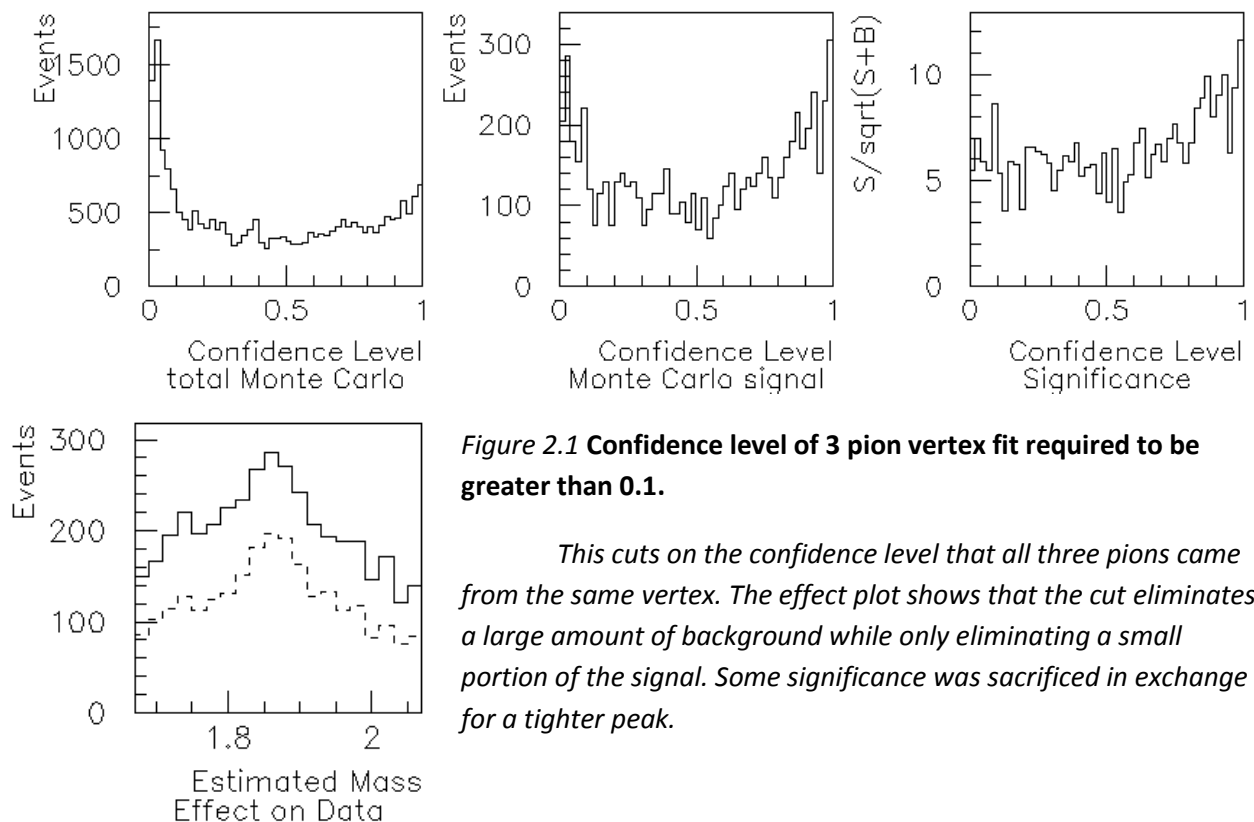
1.4 Monte Carlo Simulation of Experiment

A modified version of Pythia 6.127 was used in this analysis to generate Monte Carlo data [8]. A problem in an earlier incarnation of this analysis which only simulated D decays was that it produced a branching ratio closer to two, when one was expected. In order to see if the problem was in using an incomplete simulation of the entire E831 data set, we sought to generate enough simulated data to reproduce all the charm particles produced by E831 in all the known decay modes with many times the statistics of the actual data. To tailor the Monte Carlo to the needs of this analysis, several output parameters associated with each Monte Carlo simulation were saved to indicate if the generated event started from a charged D meson and ended in 3 pions of the correct corresponding charges and one K_L. To get more simulated events, we developed a method to use the E831 code base on a more recent linux distribution so that simulated data could be generated on several modern computers at a time. The Monte Carlo simulation was then run across 13 compute nodes for 4 days at Vanderbilt's ACCRE cluster computing center. In all, thirteen times the E831 data set was generated so that random fluctuations in the Monte Carlo data would be $\frac{1}{\sqrt{13}} \approx \frac{1}{3.6}$ as large as fluctuations in the experiment data. The large amount of data generated was then moved to a hard drive in the Vanderbilt Center for Heavy Ion and Particle Physics. This data was then skimmed for events which passed preliminary cuts into a smaller set of files which could be examined relatively quickly.

2 Candidate Reconstruction and Selection

We reconstruct decays of both D^+ and D^- into the $K^0_L \pi^+ \pi^- \pi^+$ and $K^0_L \pi^- \pi^+ \pi^-$ final states respectively from the track information using a candidate driven vertex algorithm. Given a candidate, cuts are applied based on its particle identification, geometry, and energy. A data cut is a requirement that a characteristic of a reconstructed event satisfies a criterion. Effective cuts specify criteria which favor signal events relative to background. To identify the particles, the CITADL[3] algorithm returns the relative likelihood of a Cherenkov detected particle satisfying the electron, pion, kaon, or proton hypotheses based on the individual firing patterns of all 300 cells of the C1, C2, and C3 Cerenkov counters. This likelihood is returned in the form of a χ^2 like variable which is calculated as $W_i = -2\sum_j^{cell} log\, P_j$ for W_e, W_π, W_K and W_p; P_j is the probability of the observed outcome (on or off) for the j'th cell of the Cherenkov detector under each of the 4 particle hypothesis. For each charged particle, $W_p - W_{min} < 5$ was required, effectively requiring the pion hypothesis to be very likely. This cut was not optimized, but was taken directly from an earlier set of cuts applied by Dr. Will Johns to investigate $D^\pm ->$ $K^0_S \pi^\pm \pi^+ \pi^-$.

The next several pages show the efficacy of several cuts to clean up the signal based on the event geometry and energy. For each plot of the Monte Carlo signal and background shown across a range of cut values ("signal" is $D^\pm -> K^0_L \pi^\pm \pi^- \pi^+$ in these plots), all other cuts were held constant and the mass estimate was required to be within 1.87±0.2 GeV/c^2, the D^+ mass.

Figure 2.1 **Confidence level of 3 pion vertex fit required to be greater than 0.1.**

This cuts on the confidence level that all three pions came from the same vertex. The effect plot shows that the cut eliminates a large amount of background while only eliminating a small portion of the signal. Some significance was sacrificed in exchange for a tighter peak.

Figure 2.2 **Separation between primary vertex and secondary vertex divided by the error of the distance estimate > 30.**

The D meson is created at the primary vertex. It then continues to travel for about a cm before decaying at a location called the secondary vertex. This cut requires that the primary and secondary are adequately separated so that particles from one vertex are not confused as having come from the other. The "Effect on Data" plot

shows the difference in the number of events between the >20 cut and the >30 cut. When the separation/error is >20, there is a clear peak near 1.73 GeV/c². The difference between the D meson mass of 1.87 GeV/c² and 1.73GeV/c² corresponds to the mass of a pion. Therefore, the peak possibly arises from a reconstructed $D^0 \to K^0_L \pi^+\pi^- \pi^+\pi^-$ decay in which one pion was not detected. The plot shows that increasing the separation reduces the frequency of this enhancement.
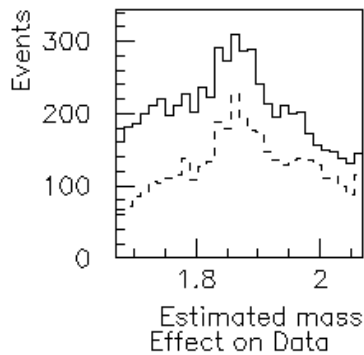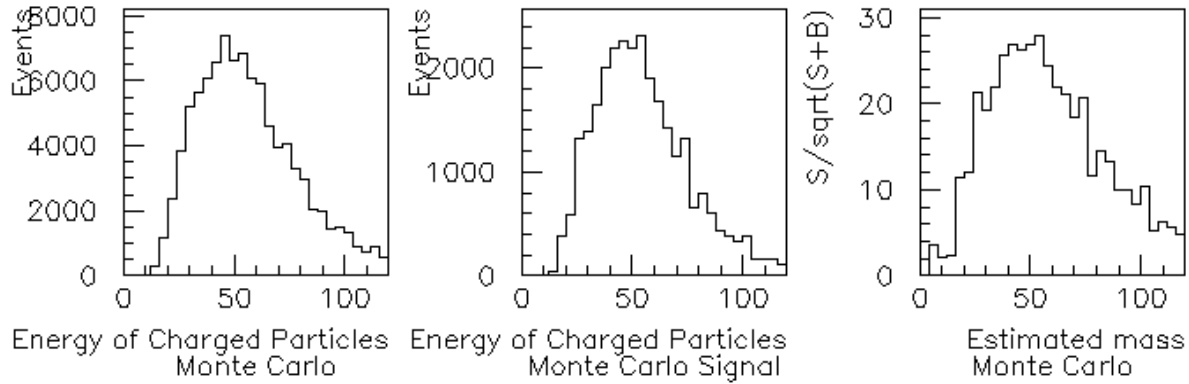

Energy of Charged Particles
Monte Carlo

Energy of Charged Particles
Monte Carlo Signal

Estimated mass
Monte Carlo

Estimated mass
Effect on Data

Figure 2.3 **Total Energy of Charged Particles > 40 GeV**

Requiring the sum of the energy of the charged particles to be greater than 40 GeV removes a large portion of background data with a mass lower than 1.87 GeV/c².
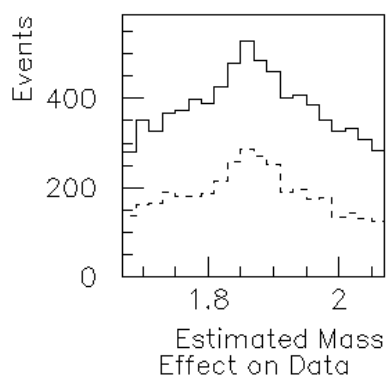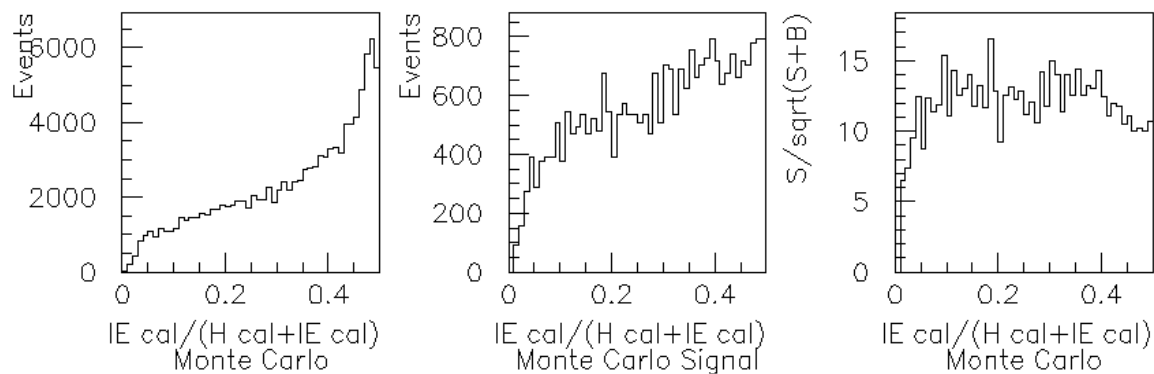
Figure 2.3 **The ratio of energy deposited in the inner electro-magnetic calorimeter/(energy deposited in the hadron calorimeter plus the inner electro-magnetic calorimeter) <0.4**

Pions are charged and thus may deposit some energy in the electromagnetic calorimeter, but both pions and kaons are hadronic particles which deposit the bulk of their energy in the hadron calorimeter. As the top left two plots show, a relatively large amount total Monte Carlo data is binned in the >0.4 region, but a relatively small amount of signal is binned in the same region.
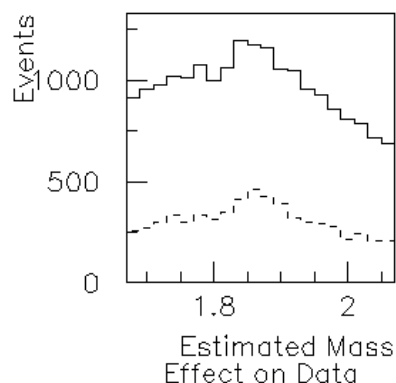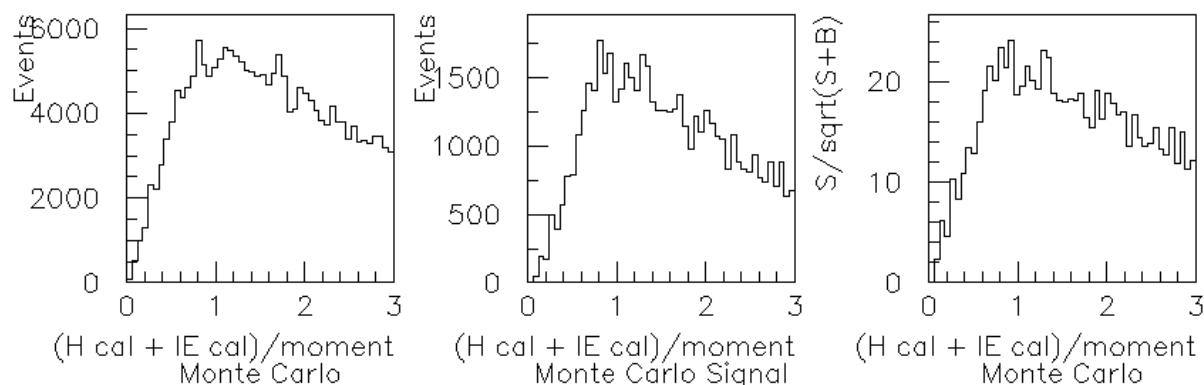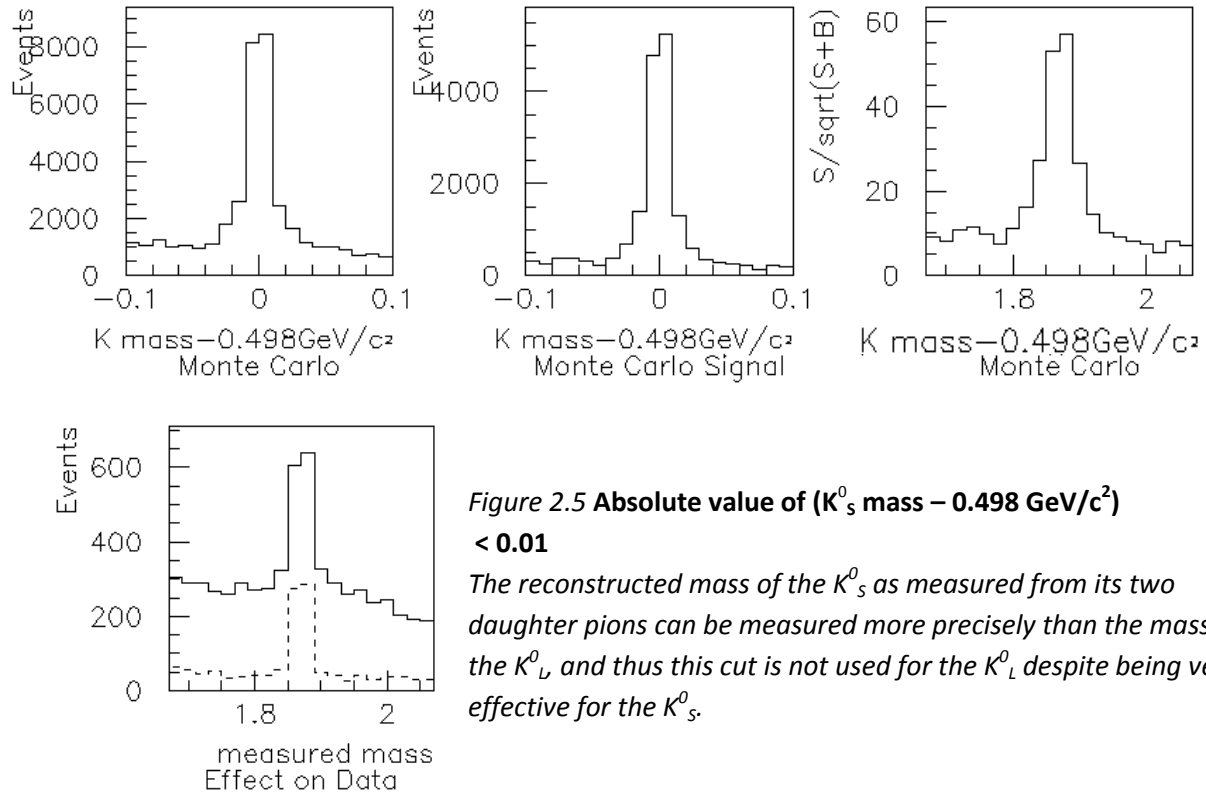

Figure 2.4 **Ratio of Energy Deposited in Calorimeter to the** *Momentum of the Decay Products must be between 0.5 and 2*

The masses of the decay products are small relative to their momentum. Therefore the ratio of energy to momentum should be near 1. The plot of the signal events shows a steeper drop in the number of events on either side of the restriction than is shown in the histogram of the total data.

Unlike the figures above, Figure 2.5 shows a histogram of $D^{\pm} \to K^0_S \pi^{\pm} \pi^- \pi^+$ events. These events passed the cuts shown in Figure 2.1-2.3, a binary cut for whether or not the event is consistent with the production of a K^0_S, and the cut shown below.

Figure 2.5 **Absolute value of (K^0_S mass – 0.498 GeV/c^2)**
< 0.01
The reconstructed mass of the K^0_S as measured from its two daughter pions can be measured more precisely than the mass of the K^0_L, and thus this cut is not used for the K^0_L despite being very effective for the K^0_S.

3 Estimating the Signal in the Data

We want to find out now if the more complete simulation produces a ratio of the kaon decay modes closer to one. To find the branching ratio of $D^{\pm} \to K^0_L \pi^{\pm} \pi^+ \pi^-$ to $D^{\pm} \to K^0_S \pi^{\pm} \pi^+ \pi^-$, an estimate of the number of actual signal events is needed for each histogram of data which passed the cuts. The signal in the $D^{\pm} \to K^0_L \pi^{\pm} \pi^+ \pi^-$ histograms are estimated by independently scaling the Monte Carlo signal events and the Monte Carlo background events to best fit the histogram of the experiment data. This was ideal because these histograms have a relatively complicated shape. The signal in the $D^{\pm} \to K^0_S \pi^{\pm} \pi^+ \pi^-$ histograms was estimated by fitting a line plus a Gaussian curve to the histogram. This could be done because the signal is cleanly separated from the background.

3.1 $D^{\pm} \to K^0_L \pi^{\pm} \pi^+ \pi^-$ Events

To estimate the amount of signal in the remaining data, the Monte Carlo signal and background are scaled individually to fit the data histogram. The estimated amount of signal in the data histogram is the number of events in the Monte Carlo signal histogram times its scaling coefficient. In each plot below, the histogram plus error bars show the number of events per bin and the estimated error of each bin.

The superimposed line graphs show the error margins of the scaled Monte Carlo to the data, with the scaling error and statistical error added in quadrature. No error estimates are given in this analysis of the total number of signal events in the experiment data(we ran out of time to do the complete error analysis). The error margins of the line graph and histogram are accurate, but a mistake in the way the fitting algorithm estimated the total error was not noticed until after the ACCRE computer cluster which contained the files used for the analysis was shut down.
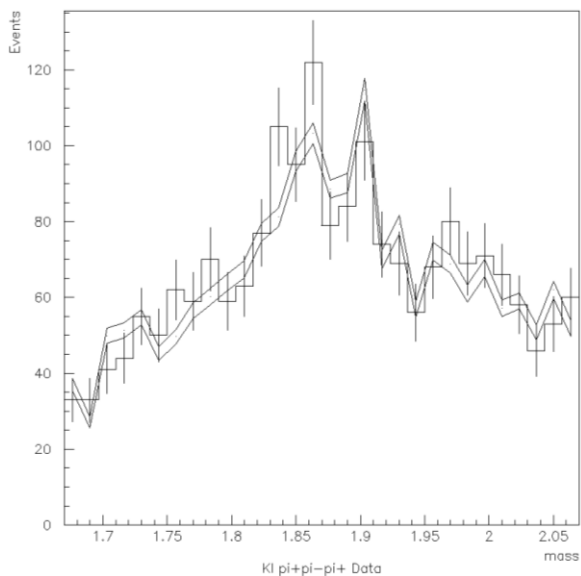

KI pi+pi−pi+ Data

Figure 3.1 This table shows the result of fitting the Monte Carlo signal and data to the experiment data. The ratio of estimated experiment signal to Monte Carlo signal is: 567/13,039 = 0.0435

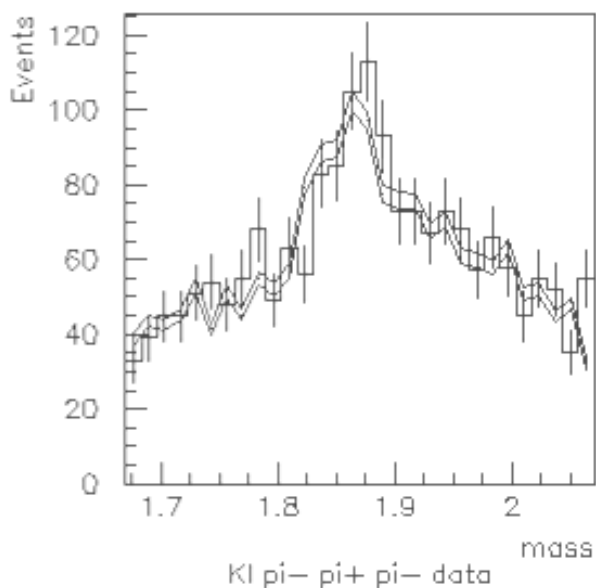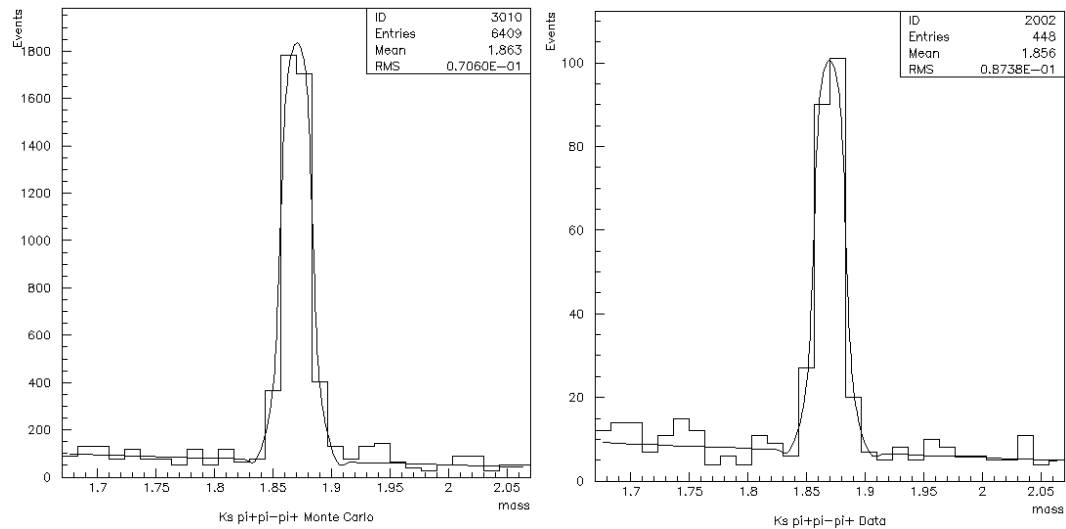| Monte Carlo Decay Process	Number of Monte Carlo Events	Scaling Coefficient	Scaled number of Monte Carlo Events
Background	26,819	8.2705 E-2	2218
$D^+ \rightarrow K^0_L \pi^+ \pi^- \pi^+$	13,039	4.350 E-2	567
		Number of Experiment Events	2,783

KI pi− pi+ pi− data

Figure 3.2 This table shows the result of fitting the Monte Carlo signal and data to the experiment data. The ratio of estimated experiment signal to Monte Carlo signal is: 501/7995 = 0.0627
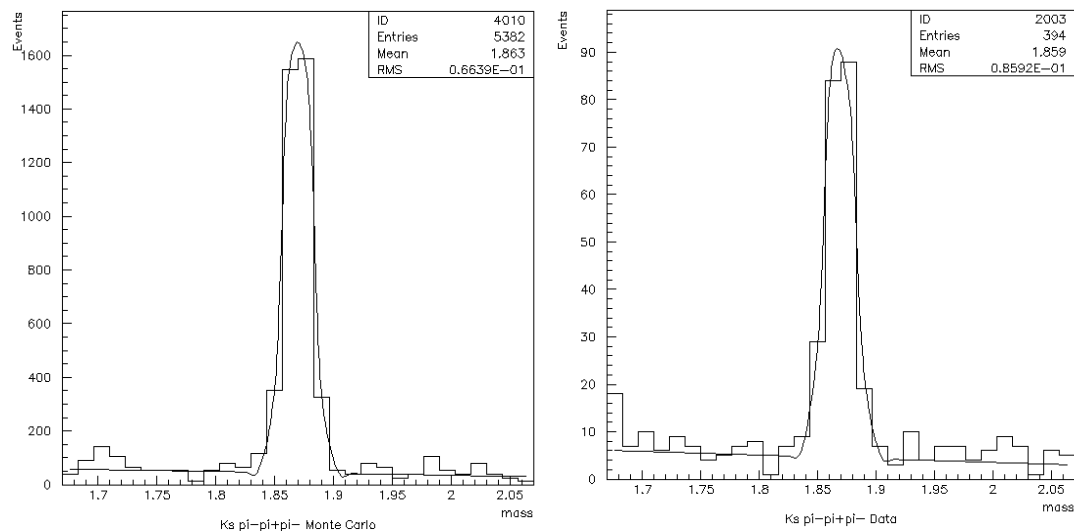
Monte Carlo Decay Process	Number of Events	Scaling Coefficient	Scaled number of Monte Carlo Events
Background	24,622	8.2367 E-2	2028
$D^- \rightarrow K^0_L \pi^- \pi^+ \pi^-$	7,995	6.2613 E-2	501
		Number of events in experiment data	2,604

3.2 D$^\pm$ -> K^0_S $\pi^\pm$ π^+ π^- Events

For both the Monte Carlo data histogram and the experiment data histogram, the number of signal events and background events are estimated as the area beneath the Gaussian and the line fit to the data, respectively. The histograms and fits of the Monte Carlo data and the experiment data are shown below:

With cuts designed to leave only D$^+$ -> K^0_S π^+ π^- π^+ events, there were 4295 ± 66 signal events and 237 ± 15 signal events according to the Gaussian fits shown above in the Monte Carlo data and experiment data respectively. The ratio of data signal to Monte Carlo signal is: 5.518 * 10^{-2}± 3.594 * 10^{-3}.

According to the gaussian fits shown above there were 4050 ± 64 signal events and 257 ± 16 signal events in the Monte Carlo data and experiment data respectively, where a signal event is D$^-$ -> K^0_S π^- π^+ π^-. The ratio of data signal to Monte Carlo signal: 6.356 * 10^{-2} ± 4.083 * 10^{-3}.

3.3 Branching Ratio

The Monte Carlo program assumed the branching ratio of K^0_L to K^0_S to be one. To test this, the ratio of experiment signal to Monte Carlo signal of the $D^\pm \to K^0_L \pi^\pm \pi^+ \pi^-$ decays are averaged, the ratio of experiment signal to Monte Carlo signal of the $D^\pm \to K^0_S \pi^\pm \pi^+ \pi^-$ decays are averaged, and the ratio of the two gives the experimentally determined branching ratio.

$$\frac{(D^+ \to K^0_L \pi^+ \pi^+ \pi^-) + (D^- \to K^0_L \pi^- \pi^+ \pi^-)}{2} \div \frac{(D^+ \to K^0_S \pi^+ \pi^+ \pi^-) + (D^- \to K^0_S \pi^- \pi^+ \pi^-)}{2} =$$

$$\frac{5.31 * 10^{-2}}{5.94 * 10^{-2}} = 0.89$$

Our hypothesis that a complete simulation of the experimenal data needs to be used for this analysis is somewhat justified with our result. The ratio at first glance is different than the previous value of ~2 seen using a more targeted simulation. Unfortunately, the error margins of this estimate cannot be given and so the statistical significance of the result remains in question for now.

4. Further Work

4.1 Statistical Error Estimates

In order to assess the statistical significance of the branching ratio found here, the error of the estimate of the amount of signal in the histograms of the experimental data must be propagated to the branching ratio.

4.2 Systematic Errors

For $D^+ \to K^0_L \pi^+ \pi^- \pi^+$, Monte Carlo background has a broad peak at 750 events, except for one mass bin which has 1000 events as shown in figure 4.1. The bin is $250/\sqrt{750} > 9$ standard deviations from the rest of the data. This seems to indicate that there is a bug in the Monte Carlo program causing an event in that bin to occur excessively.
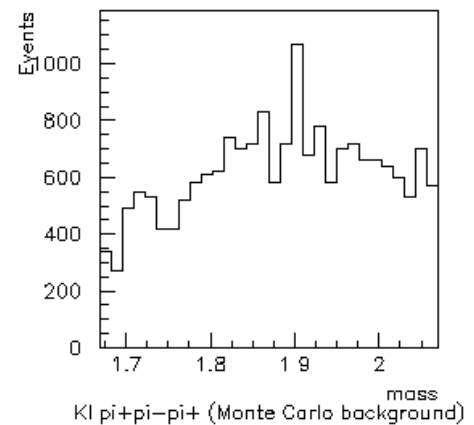

Figure 4.1 Monte Carlo Background

4.3 Peak at 1.9 GeV/c²

Both the Monte Carlo and the experimental data have a peak at 1.9 GeV/c² in the histogram of $D^+ \to K^0_L \pi^- \pi^+ \pi^-$ decays. The cause of this peak may be worth investigating.

Bibliography

[1] E687 Collab., P.L. Frabetti *et al.*, Nucl. Instrum. Methods Phys. A 320 (1992) 519.

[2] Link, J., M. Reyes, P. Yager, J. Anjos, I. Bediaga, C. Gobel, J. Magnin, A. Massafferri, J. Demiranda, and I. Pepe. "The Target Silicon Detector for the FOCUS Spectrometer." *Nuclear Instruments and Methods in Physics Research Section A: Accelerators, Spectrometers, Detectors and Associated Equipment* 516.2-3 (2004): 364-76. Print.

[3] Link, J., M. Reyes, P. Yager, J. Anjos, I. Bediaga, C. Gobel, J. Magnin, A. Massafferri, J. Demiranda, and I. Pepe. "Cherenkov Particle Identification in FOCUS." *Nuclear Instruments and Methods in Physics Research Section A: Accelerators, Spectrometers, Detectors and Associated Equipment* 484.1-3 (2002): 270-86. Print.

[4] C. Amsler et al.. (2008): Particle listings – D±

[5] C. Amsler et al.. (2008): Particle listings – π±

[6] J. Beringer et al. (2012): Particle listings – K^0_S

[7] J. Beringer et al. (2012): Particle listings – K^0_L

[8] T. Sjostrand, Computer Physics Commun. 82 (1994) 74.